

Pump-coupled micromasers: Entangled trapping states of nonlocal fields

Pál Bogár and János A. Bergou

*Department of Physics and Astronomy, Hunter College of the City University of New York
695 Park Avenue, New York, New York 11021*

(Received 21 July 1994)

A single beam of excited two-level atoms couples two micromasers in a series. It is shown that in the absence of dissipation the possible steady states of their fields are superpositions, of two-field trapping number states. Which one is realized depends upon the initial state of the fields and the interaction parameters, $g'\tau'$ and $g''\tau''$, of the two cavities. A large number of these trapping states are pure quantum states, some of them showing entanglement of the two nonlocal micromaser fields of the form $|N, N+M\rangle \pm |N+M, N\rangle$. Here, N and $N+M$ are arbitrary trapping numbers that belong to disconnected blocks of the photon number space and M specifies the order of correlation between the fields. The time evolution of the system toward steady states is investigated numerically, mainly concentrating on the production of pure entangled trapping states of the form discussed earlier. We describe a special procedure to amplify a number state, $|N, N\rangle$, into such states that is based on conditions regarding the interaction parameters. In principle, N and M can be made arbitrarily large resulting in a steady-state nonlocal quantum superposition of distinct macroscopical fields (nonlocal "Schrödinger cat"). We also present a solution of the standard master equation of a damped harmonic oscillator at finite temperature and apply it to study the effect of dissipation on the production of entangled trapping states at regular and Poissonian pump statistics. It is found that although the entanglement does not survive at a steady state it can build up in the short-time transient regime when cavity losses and the number of thermal photons are not too large. In this small-loss (large N_{ex}) regime the quantum correlation between the micromaser fields decays into a steady-state classical superposition at a rate that depends on the cavity lifetime and the difference (or order of correlation), M , between the superposed photon numbers. In the large-loss (small N_{ex}) regime, however, no transient correlation can be produced and the photon statistics spreads out towards a vacuum for increasing losses. The system undergoes a transition from an uncorrelated to a correlated behavior when the pumping parametrized by N_{ex} exceeds the threshold between the large- and small-loss regimes. Thermal photons enhance the decay of the correlation and by coupling the disconnected blocks of the photon number space they populate the trapping number states of adjacent blocks. However, it is shown that the production of transient entanglement is not significantly affected by either thermal radiation or pumping fluctuations. The experimental realization of the entanglement of nonlocal micromaser fields employing these two-field trapping states of small photon numbers is shown to be feasible in the short-time transient regime using the presently available high- Q cavities and low temperatures, and could be possible on the macroscopic scale in the near future.

PACS number(s): 42.50.Dv, 42.52.+x

I. INTRODUCTION

The preparation of macroscopic quantum superpositions is of considerable interest in quantum optics. The principle of superposition is one of the most significant contradictions between quantum and classical physics, the implications of which are particularly astonishing on the macroscopic level. This problem has been exploited in many different systems, for example, in the micromaser [1] that is one of the fundamental systems of this field of research [2]. Its importance is based upon its genuine quantum nature exhibiting all the important quantum phenomena of matter-light interaction, and at the same time its theoretical tractability [3,4] and experimental feasibility [5,6]. Some of the most important examples include collapse and revival of the Rabi nutation [7], generation of nonclassical photon statistics [1–5,8] to the extreme cases of number states [9], trapping states [10], and macroscopic coherent superpositions of its single-mode radiation field [1].

The present paper further extends this respectable list of nonclassical effects, studying the quantum correlations between two micromasers coupled in series by the common pumping atomic beam (see Fig. 1) and investigating the production of entangled states and nonlocal superpo-

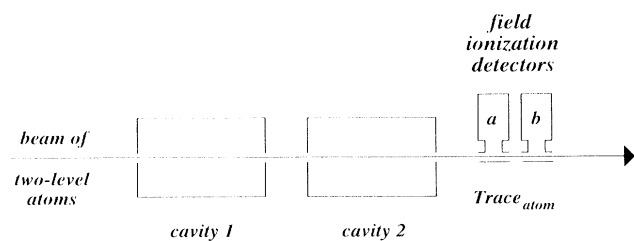


FIG. 1. Schematic arrangement of two micromasers coupled by a beam of two-level atoms, the state of which is measured after the interaction by the field ionization detectors without selecting a particular result.

sitions of the two micromaser fields [11–13]. One way to prepare such quantum fields is to perform conditional measurements on the atoms emerging from the interaction cavity as discussed in Ref. [12]. However, in this paper we show that the system can be driven into pure entangled trapping states of the two fields without performing conditional measurements. In fact, it is possible to generate arbitrary quantum superpositions of two nonlocal micromaser fields of the form of $|N, N+M\rangle \pm |N+M, N\rangle$ at steady state in the absence of dissipation, where N and $N+M$ satisfy the trapping conditions in the two micromasers. We describe a two-step procedure to generate these states from the number state, $|N, N\rangle$, that is based on special conditions regarding the interaction parameters, $g'\tau'$ and $g''\tau''$, of the two cavities. Since quantum superpositions and trapping states are known to be very fragile against dissipations [14] and thermal effects [8], the question arises of how well our procedure performs in the presence of cavity losses and thermal radiation. Applying our solution of the standard master equation of a damped harmonic oscillator, it is shown that these entangled trapping states can be produced in the transient regime when the pumping, N_{ex} , exceeds a certain threshold established by the losses. We also find that finite temperature and pumping fluctuations do not significantly modify the transient buildup of the correlation between the fields. According to our estimate, experimental realization of transient entanglement of nonlocal micromaser fields is feasible using presently available facilities utilizing special configurations of two-field trapping states such as, for example, the one above.

The paper is organized as follows. Section II introduces the steady-state solution of the system in the absence of dissipation, distinguishing between mixed and pure quantum states. In Sec. III the time evolution toward steady states is studied, especially the pure entangled states of the above form. The effects of dissipation,

thermal radiation, and pump fluctuations on the buildup of entangled trapping states are investigated in Sec. IV. The summary and conclusions are presented in Sec. V.

II. STEADY-STATE BEHAVIOR IN THE ABSENCE OF DISSIPATION

We consider two micromasers pumped by a monoenergetic beam of excited two-level atoms going through cavity 1 first and then through cavity 2 with no time delay between the cavities (see Fig. 1). The density of the atomic beam is low enough in order to have at most one atom at a time inside the cavities. The effect of dissipation is ignored in the present section, it will be taken into account later on. The state of the atoms is measured after the interaction in cavity 2, but we do not select a particular result. We assume 100% detection efficiency for the field ionization detectors measuring the state of the outgoing atoms in order to have each atom measured after the interaction. The state of the fields is described by the reduced density operator obtained by tracing out over the atomic states. This tracing operation is sometimes referred to as a nonselective measurement [15]. The evolution of the system is governed by the Jaynes-Cummings operators, U' and U'' , during the atom-field interactions in cavities 1 and 2, respectively. At the instant when the k th atom leaves cavity 2 the field density operator reduces to

$$\rho^{(k)} = \text{Tr}_{\text{atom}} [U'' U' \rho^{(k-1)} \rho_{\text{atom}} U'^{\dagger} U''^{\dagger}], \quad (2.1)$$

where ρ_{atom} is the atomic and $\rho^{(k-1)}$ is the field-density operator at the instant when the k th atom enters cavity 1. In the number representation

$$\rho_{n_1, m_1}^{(k)} = \langle n_1, n_2 | \rho^{(k)} | m_1, m_2 \rangle, \quad (2.2)$$

this reads as

$$\begin{aligned} \rho_{n_1, m_1}^{(k)} = & \rho_{n_1, m_1}^{(k-1)} C'_{n_1+1} C'_{m_1+1} C''_{n_2+1} C''_{m_2+1} + \rho_{n_1-1, m_1-1}^{(k-1)} S'_{n_1} S'_{m_1} C''_{n_2} C''_{m_2} + \rho_{n_1-1, m_1-1}^{(k-1)} S'_{n_1} S'_{m_1} S''_{n_2+1} S''_{m_2+1} \\ & + \rho_{n_1, m_1}^{(k-1)} C'_{n_1+1} C'_{m_1+1} S''_{n_2} S''_{m_2} - \rho_{n_1, m_1-1}^{(k-1)} C'_{n_1+1} S'_{m_1} C''_{n_2+1} S''_{m_2+1} + \rho_{n_1-1, m_1}^{(k-1)} S'_{n_1} C'_{m_1+1} C''_{n_2} S''_{m_2} \\ & - \rho_{n_1-1, m_1}^{(k-1)} S'_{n_1} C'_{m_1+1} S''_{n_2+1} C''_{m_2+1} + \rho_{n_1, m_1-1}^{(k-1)} C'_{n_1+1} S'_{m_1} S''_{n_2} C''_{m_2}. \end{aligned} \quad (2.2)$$

Here, $S'_{n_1} \equiv \sin(g'\tau'\sqrt{n_1})$ and $S''_{n_2} \equiv \sin(g''\tau''\sqrt{n_2})$, C'_{n_1} and C''_{n_2} stand for the cosine functions of the corresponding arguments, g' and g'' are the atom-field coupling constants, and τ' and τ'' are the interaction times in cavities 1 and 2, respectively.

Representing the four-dimensional density matrix as a supermatrix of matrices where one matrix is specified by the photon numbers of the first field, (n_1, m_1) , and one element of this matrix is given by those of the second

field, (n_2, m_2) , Eq. (2.2) tells us that any matrix element, (n_1, m_1, n_2, m_2) , is coupled to others located along a “double square” as depicted in Fig. 2. This shows, for example, that the photon statistics [diagonal elements, (n_1, n_1, n_2, n_2)] are coupled to the coherence terms [off-diagonals, $(n_1, n_1 \pm 1, n_2 \pm 1, n_2)$], indicating the essential role of correlations in this system. The strength of the coupling is determined by the sine and cosine functions in Eq. (2.2). In the interaction picture and in the absence of

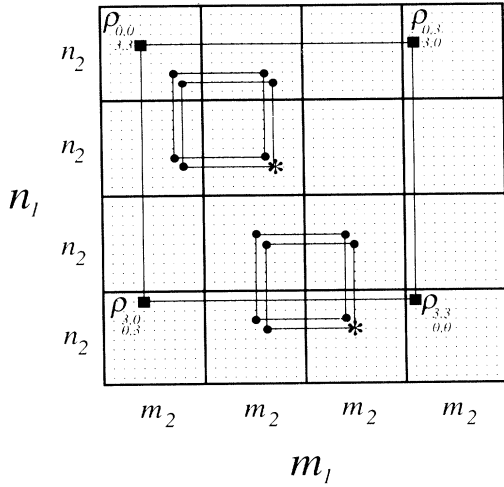


FIG. 2. The structure of the coupling between the elements of the field-density matrix arranged in the form of a supermatrix, one matrix of which is given by the photon numbers of the first micromaser, n_1 and m_1 , while the elements of this matrix are given by n_2 and m_2 of the second micromaser. (The indices, n_1 and n_2 , increase downward and m_1 and m_2 to the right.) Two examples show how a matrix element depicted by a star is coupled according to Eq. (2.2) to others located along the double square shown by the solid circles. The four solid rectangles give an example for the structure of a pure state given by $|0,3\rangle \pm |3,0\rangle$ (apart from a normalization factor).

dissipation the density operator does not evolve during the time interval t between the atoms. Thus, successive iterations of Eq. (2.2) yield the stroboscopic time evolution of the fields. This will be studied in the next section

by numerically evaluating Eq. (2.2) for a stream of atoms. It can be seen from Eq. (2.2) that for steady states of the fields one needs

$$C'_{N_1+1} C'_{M_1+1} C''_{N_2+1} C''_{M_2+1} = 1, \quad (2.3)$$

which is the trapping condition satisfied by any combinations of any four numbers N_1 , M_1 , N_2 , and M_2 for each of which $g\tau\sqrt{N+1} = q\pi$, where q is an integer and N is any of the four numbers. Thus, in the absence of dissipation, the only possible steady states of the system are the superpositions of these two-field trapping number states satisfying Eq. (2.3). They include both mixed and pure quantum states of the fields as can be seen from the supermatrix picture. Populating, for example, the diagonal trapping number states only will provide us with mixed states of no correlation between the fields, while also populating the off-diagonal ones will result in correlations between the micromasers and in some cases of pure quantum states. An example is given in Fig. 2 representing the pure quantum state, $|0,3\rangle \pm |3,0\rangle$ (apart from a normalization factor), that is an entangled trapping state of the two micromaser fields for the interaction parameters, $g'\tau' = g''\tau'' = \pi$.

We want to select pure states from this broad set of steady states by applying the following factorization argument [1]. Let us assume that the initial state of the fields is given by

$$|\Psi\rangle = \sum_{n_1, n_2} \Psi_{n_1, n_2} |n_1, n_2\rangle. \quad (2.4)$$

We require this state to be a steady state of the fields. Interacting with an atom initially in its upper state, $|a\rangle$, the atom-field system under the Jaynes-Cummings dynamics evolves into the state given by

$$|\Phi\rangle = \sum_{n_1, n_2} \Psi_{n_1, n_2} [(C'_{n_1+1} C''_{n_2+1} |n_1, n_2\rangle - S'_{n_1+1} S''_{n_2} |n_1+1, n_2-1\rangle) |a\rangle - i(C'_{n_1+1} S''_{n_2+1} |n_1, n_2+1\rangle + S'_{n_1+1} C''_{n_2} |n_1+1, n_2\rangle) |b\rangle]. \quad (2.5)$$

The requirement that the fields remain in the same pure state after the interaction implies that $|\Phi\rangle$ must factorize into a tensor product of the initial pure state of the fields given by Eq. (2.4) and a pure state of the atoms as

$$|\Phi\rangle = e^{i\theta} |\Psi\rangle \otimes (\alpha |a\rangle + \beta |b\rangle), \quad (2.6)$$

where α , β , θ are independent of n_1, n_2 and $|\alpha|^2 + |\beta|^2 = 1$. Comparing Eqs. (2.5) and (2.6) we readily find

$$e^{i\theta} \alpha \Psi_{n_1, n_2} = \Psi_{n_1, n_2} C'_{n_1+1} C''_{n_2+1} - \Psi_{n_1-1, n_2+1} S'_{n_1} S''_{n_2+1}, \quad (2.7)$$

$$e^{i\theta} \beta \Psi_{n_1, n_2} = -i(\Psi_{n_1, n_2-1} C'_{n_1+1} S''_{n_2} - \Psi_{n_1-1, n_2} S'_{n_1} C''_{n_2}). \quad (2.8)$$

It is apparent from Eq. (2.8) that for a steady state we need $\beta=0$, and consequently $\alpha = \pm 1$ and $e^{i\theta} = \pm 1$, i.e., atoms to leave cavity 2 in their upper state. This implies that they need to be in their upper state before, between, and after the cavities at steady state. Hence, it follows from Eq. (2.7) that the necessary condition for a nonzero field amplitude, $\Psi_{N_1, N_2} \neq 0$, is

$$C'_{N_1+1} C''_{N_2+1} = \pm 1, \quad (2.9)$$

which is satisfied by the two-field trapping conditions

$$g'\tau'\sqrt{N_1^{(p)}+1} = p\pi, \quad (2.10)$$

$$g''\tau''\sqrt{N_2^{(q)}+1} = q\pi. \quad (2.11)$$

Any combination of $N_1^{(p)}$ and $N_2^{(q)}$ determines a point in

the photon number space, n_1-n_2 , where a nonzero amplitude, $\Psi_{N_1^{(p)}, N_2^{(q)}} \neq 0$, can arise, resulting in the most general steady states of the fields given by

$$|\Psi\rangle = \sum_{p,q} \Psi_{N_1^{(p)}, N_2^{(q)}} |N_1^{(p)}, N_2^{(q)}\rangle. \quad (2.12)$$

There are no other pure steady states of the system. It is apparent that the solution of Eq. (2.3) provides a broader set of trapping states including the ones given by Eq. (2.12) as well as those for which a pure state vector does not exist. In the case of $g\tau \equiv g'\tau' = g''\tau''$ Eq. (2.12) reduces to the combination of a single set of trapping photon numbers. Choosing, for example, $g\tau = \pi/\sqrt{5}$, the possible trappings occur at photon numbers $N^{(p)} = 4, 19, 44, \dots$ for $p = 1, 2, 3, \dots$, resulting in trapping states such as number states, $|4, 4\rangle$ or $|19, 19\rangle$, and a combination thereof, or such as entangled states exhibiting strong correlation between the two nonlocal micromaser fields [12,13], for example,

$$|\Psi\rangle = \frac{1}{\sqrt{2}} (|4, 19\rangle + |19, 4\rangle). \quad (2.13)$$

Going back to the supermatrix picture we find that the ensemble of possible trapping number states determined by the interaction parameters, $g'\tau'$ and $g''\tau''$, marks the borders of disconnected blocks inside which the fields are bound to evolve. Unless finite temperature is introduced into the system (as will be studied in Sec. IV) the fields cannot reach beyond the trapping states and enter the region of another block in the supermatrix, but they must stay in the block they started in. Hence, the initial state of the fields and the interaction parameters determine

which part of the general trapping state [mixed, Eq. (2.3) or pure, Eq. (2.12)] the system will evolve into. The dynamics of the fields will be studied in the next section where, in particular, we are going to describe a procedure that takes advantage of the disconnected structure of blocks in the photon number space and generates various nonlocal superpositions of trapping states [such as Eq. (2.13)] starting from initial fields that overlap several (two) blocks simultaneously.

III. TIME EVOLUTION TOWARD TRAPPING STATES IN THE ABSENCE OF DISSIPATION

We have seen in the preceding section in the absence of dissipation the steady state of the fields consists of various ensembles of two-field trapping number states, some of which exhibit pure entanglement of the two nonlocal micromaser fields. In this section we are investigating typical time evolutions of the fields toward steady states, considering various initial conditions and concentrating mainly on the production of pure entangled states. We compute the density matrix for a stream of atoms by numerically iterating Eq. (2.2).

A. Uncorrelated initial states

As a first example let us start the fields from vacuum and set $g\tau = 0.5$. It can be seen from Fig. 3 that the field in the second micromaser experiences an initial flip: after an initial growth it falls back to vacuum around the 20th atom. This “second threshold” corresponds to a complete depletion of the upper atomic level by the first mi-

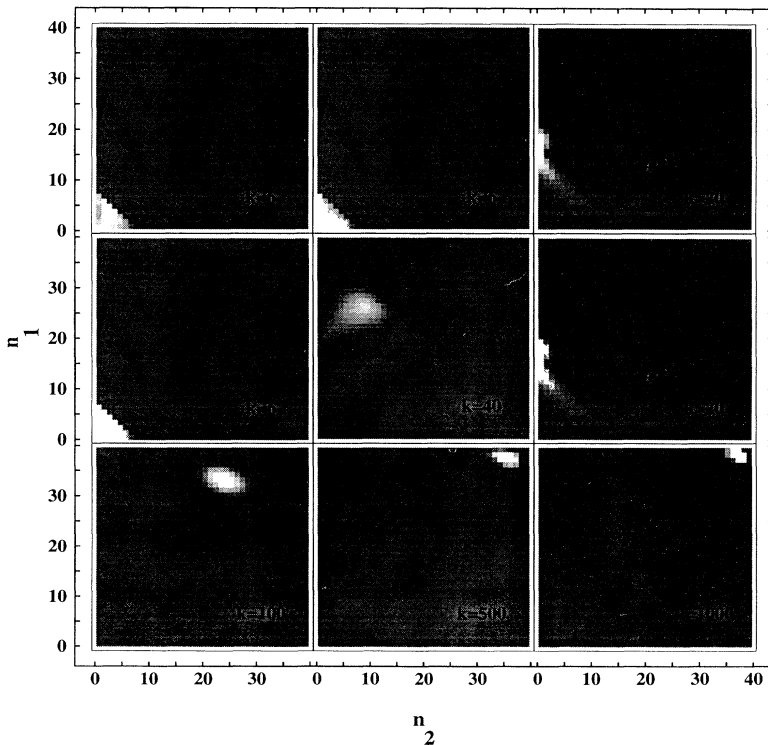


FIG. 3. Density plot of the time evolution of the photon statistics of the fields started from vacuum applying $g\tau = 0.5$. Brighter points correspond to higher probabilities, the gray level to zero, and numbers k in the figure are the atom numbers. After an initial flip lasting until $k \approx 20$ the fields evolve toward $n_1 \approx n_2 \approx 38$ in a well-localized structure.

micromaser and it is studied in Ref. [16] in detail. The flip is longer in time and sweeping over larger photon numbers for smaller $g\tau$'s, while it is shorter and will even disappear for larger parameters. After the flip the fields evolve toward $n_1 = n_2 \cong 38$, which is close although not exactly equal to the π -trapping point, $N_1 = 38.478$. This "pseudotrapping" point attracts the fields to spend a long time in its vicinity, but then the system moves on. This can be seen from another example depicted in Figs. 4(a) and 4(b), where $g\tau = 3\pi/\sqrt{29}$ resulting in the "pseudotrapping" points attracting the fields to $N_1 = 2.222$ and $N_2 = 11.889$, and the "true-trapping" point at $N_3 = 28$. Figure 4(a) shows that the system spends long times in the two pseudotrapping points, but then it finally evolves

into its true steady state, $|28, 28\rangle$. The evolution of the purity factor defined as $\xi^{(k)} = \text{Tr}[\rho^{(k)2}]$ as a function of atom number k is depicted in Fig. 4(b). We have obtained very similar effects including the initial flip and the attraction by pseudotrapping points when starting the fields from a single or from an incoherent mixture of number states, although in the latter case the system may evolve into a classical mixture of several trapping points belonging to different disconnected blocks of the photon number space. (We are using the terms "classical" and "incoherent" as equivalents throughout this paper.) Similarly, starting from initially uncorrelated coherent states the system simultaneously deals with several (both "pseudo-" and "true-") trapping points depending on $g\tau$.

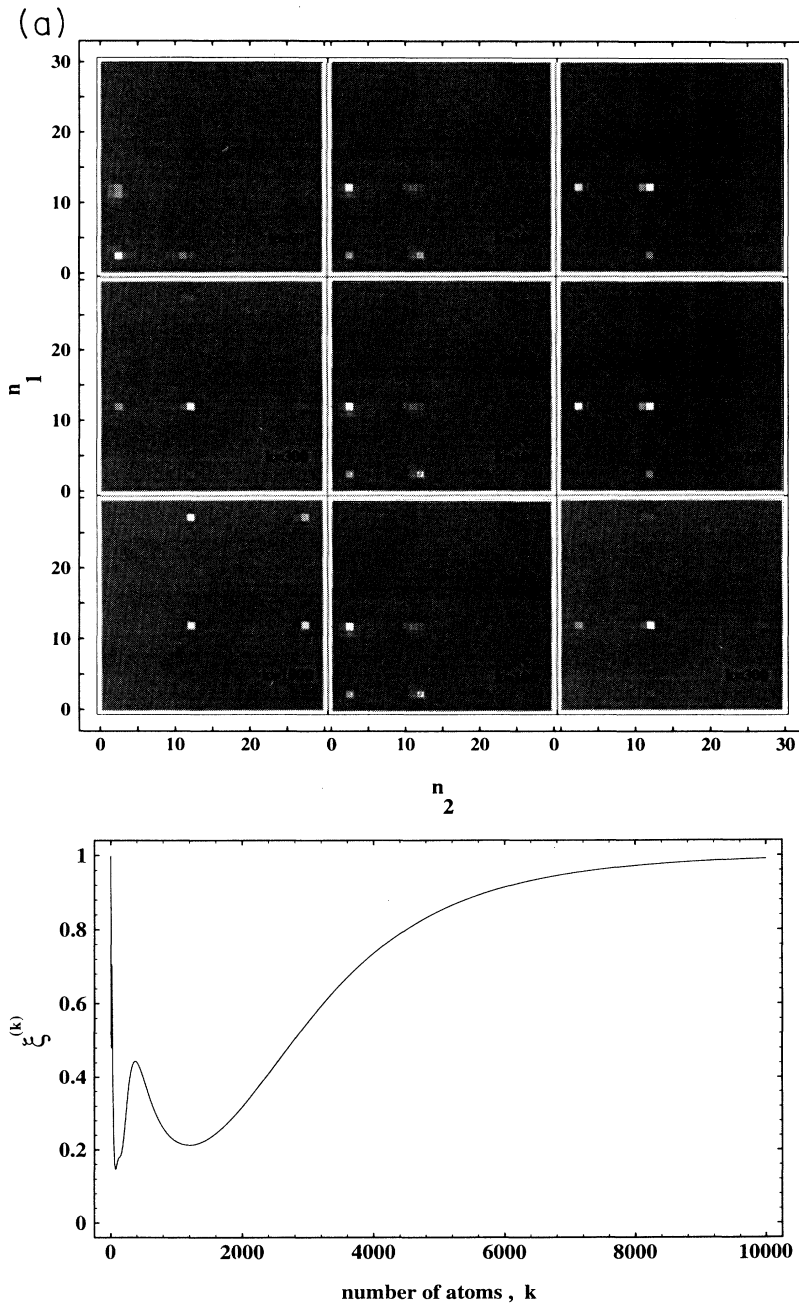


FIG. 4. (a) Density plot of the time evolution of the photon statistics of the fields started from vacuum applying $g\tau = 3\pi/\sqrt{29}$. The system spends long times in the pseudotrapping points around $N_1 \cong 2$ and $N_2 \cong 12$ and combinations thereof, until it finally evolves into the true-trapping point at $N_3 = 28$. (b) The evolution of the purity factor, $\xi^{(k)} = \text{Tr}[\rho^{(k)2}]$, as a function of the atom number k corresponding to the fields depicted in (a). The peak around $k \cong 400$ corresponds to photon statistics that are very similar to that of the number state, $|12, 12\rangle$, at the pseudotrapping point, $N_2 \cong 12$. Finally, the steady state is the number state, $|28, 28\rangle$, with purity factor of 1.

After the initial flips it finally settles down to an incoherent mixture of trapping photon numbers located at different disconnected blocks under the envelope of the initial fields, showing no correlation between the micromaser fields (this is similar to the problem discussed in Ref. [12] in detail). We could not generate pure entangled states starting from these uncorrelated initial states even if they overlapped several disconnected blocks of the photon number space.

B. Amplification of correlated states, $|\Psi\rangle_n^{(m)}$

We are going to show, however, that a correlated state of the two micromaser fields, $|\Psi\rangle_n^{(m)}$, that exhibits a structure given by

$$|\Psi\rangle_n^{(m)} = \frac{1}{\sqrt{2}}(|n, n+m\rangle \pm |n+m, n\rangle) \quad (3.1)$$

can be amplified into the pure steady state, $|\Psi\rangle_N^{(M)}$, of the same form as above, provided N and $N+M$ are trapping numbers. It should be mentioned here that, defining m th-order correlation by the nonseparability condition

$$\langle (\hat{a}_1 \hat{a}_2^\dagger)^m \rangle \neq \langle \hat{a}_1^\dagger \rangle \langle \hat{a}_2^\dagger \rangle^m, \quad (3.2)$$

where \hat{a}_1 (\hat{a}_1^\dagger) and \hat{a}_2 (\hat{a}_2^\dagger) are the field operators in micromasers 1 and 2, respectively, it is easy to show that these states, $|\Psi\rangle_n^{(m)}$, exhibit m th-order correlation. We would like to draw attention to the fact that this is a correlation between fields of two spatially separated micromasers, i.e., a *nonlocal* entanglement. The state of one of the fields can be inferred from a measurement made on the state of the other field located at a different point in space.

The amplifying procedure of an initial state, $|\Psi\rangle_n^{(m)}$, the preparation of which will be discussed later on, is based on conditions regarding the interaction parameters, $g'\tau'$ and $g''\tau''$, of the two cavities. Choosing the appropriate parameters, we want to trap photon number n in its initial value in Eq. (3.1), making $|\Psi\rangle_n^{(m)}$ overlap two different disconnected blocks in the photon number space. Thus, n is going to be a constant throughout the procedure, i.e., $N=n$, while $n+m$ located in the other block disconnected from the one of n can be amplified. Due to the structure of $|\Psi\rangle_n^{(m)}$ the roles of the two fields are interchanged in the two terms: the first and second fields are trapped only in the first and second terms, respectively. Therefore, an increase in m will result in a symmetrical amplification of the different fields in the different terms until the trapping number $N+M$ is reached, preserving the structure of the entanglement the same as in Eq. (3.1). This also implies an increase in the order of correlation trapped at the value of $m=M$ at steady state. It follows from Eq. (2.5) that since the amplitudes of the initial fields are $\Psi_{n,n+m} = \pm \Psi_{n+m,n} = 1/\sqrt{2}$ this procedure can be carried out by simultaneously satisfying two conditions given by

$$S'_{n+1} = S''_{n+1} = 0 \quad (3.3)$$

and

$$S''_n = 0. \quad (3.4)$$

The first condition most importantly ensures that a given state, $|\Psi\rangle_n^{(m)}$, gets amplified in the desired way when the atom leaves the interaction in its lower state, while together with the second one they prevent quantum states of structures different than $|\Psi\rangle_n^{(m)}$ from contributing to the state of the fields when the atom leaves in its upper state. In particular, considering the second line of Eq. (2.5) the initial amplitude, $\Psi_{n,n+m}$ ($\Psi_{n+m,n}$), allows only the first (second) term to contribute and the other one is suppressed due to Eq. (3.3). Similarly, in the first line of Eq. (2.5) only the first term contributes and the second one is suppressed for both amplitudes as a result of Eqs. (3.3) and (3.4). These two conditions imply that the interaction parameters must be integer multiples of $\pi/\sqrt{n+1}$ and π/\sqrt{n} *simultaneously*. Since this is not, in general, possible we are going to start in the following examples with concentrating on the first condition only, describing the resulting effect of mixing different structures into the evolution of the fields, and then apply the second condition approximately. It will be shown that this approximate solution for $g\tau$ works very well in the amplifying procedure and the generated states are very close to the pure entangled trapping states, $|\Psi\rangle_N^{(M)}$. We should mention here without going into details that unequal interaction parameters, $g'\tau'$ and $g''\tau''$ [both approximately satisfying Eqs. (3.3) and (3.4)], result in a reduction and ultimately a loss in the correlation and purity of the fields at steady state due to an asymmetrical amplification of the state vector. Therefore, we require $g\tau \equiv g'\tau' = g''\tau''$ in the amplifying procedure.

As the simplest example let us consider an initial state, $|\Psi\rangle_0^{(m)}$, given by Eq. (3.1) for $n=0$. It can be seen from Eq. (2.5) that detecting the first atom emerging from the interactions in the upper state, $|a\rangle$, will not change the state of the fields, $|\Psi\rangle_0^{(m)}$, (apart from a phase factor) if $g\tau = q\pi$, where q is an integer. On the other hand, detecting the lower state, $|b\rangle$, will increase m by 1 until the trapping point M is reached, and at the same time preserve $n=0$ unchanged, resulting in the state $|\Psi\rangle_0^{(m+1)}$. The tracing operation averages the two atomic paths out and the state of the fields is a statistical mixture of the two corresponding quantum states, $|\Psi\rangle_0^{(m)}$, and $|\Psi\rangle_0^{(m+1)}$, both exhibiting the form of Eq. (3.1). Similarly, for all the consecutive atoms the states of the fields during the evolution are always statistical mixtures of quantum states of the form of $|\Psi\rangle_0^{(m)}$ only; no other structures will contribute. This suggests that the system inevitably evolves into the trapping state, $|\Psi\rangle_0^{(M)}$, where M can be any trapping number $M=3, 8, 15, \dots$ depending on which disconnected block we are working in. In other words, the trajectory of the fields (i.e., the sequence of states they evolve along) consists of states like $|\Psi\rangle_0^{(m)}$ only, where m is increasing with the number of injected pumping atoms while $n=0$ is kept constant. Figure 5(a) depicts the field-density matrix for the first two atoms in the form of a supermatrix (arranged in the same way as in Fig. 2) starting from the initial state, $|\Psi\rangle_0^{(1)}$, at $g\tau = \pi$. Comparing the structure of the pure state, $|\Psi\rangle_0^{(3)}$, depicted in Fig. 2 to Fig. 5(a) it can be seen that the system

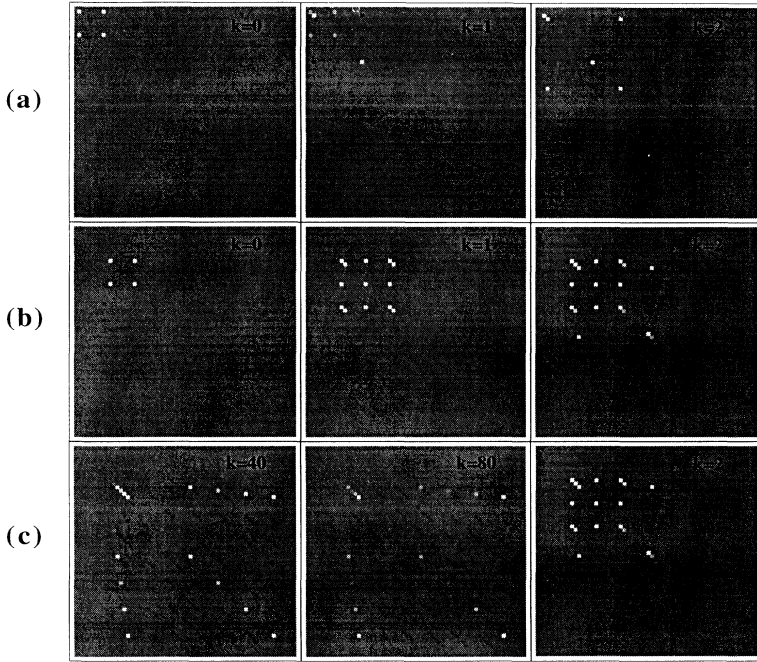


FIG. 5. Density plot of field-density matrices in the form of supermatrices discussed in Fig. 2 at atom numbers k given in the figure (dark points correspond to negative values). The initial states and applied $g\tau$'s are (a) $|\Psi\rangle_0^{(1)}$, $g\tau=\pi$, (b) $|\Psi\rangle_1^{(1)}$, $g\tau=\pi/\sqrt{2}$, and (c) $|\Psi\rangle_1^{(1)}$, $g\tau=7\pi/\sqrt{2}$. The evolution of the density matrix shows statistical mixtures of pure states of (a) $|\Psi\rangle_0^{(m)}$ for $m=1,2,3$ and (c) $|\Psi\rangle_1^{(m)}$ for $m=1,\dots,6$, resulting in pure steady states of (a) $|\Psi\rangle_0^{(3)}$ and (c) $|\Psi\rangle_1^{(6)}$. In the case of (b) other states of different structures also contribute, resulting in a mixed quantum state of the fields at steady state.

evolves along a statistical mixture of pure states, $|\Psi\rangle_0^{(m)}$, of $m=1,2,3$. Numerically iterating Eq. (2.2) for several atoms we find that the fields finally evolve into the trapping state, $|\Psi\rangle_0^{(3)}$. The solid line in Fig. 6 shows that the purity factor $\xi^{(k)}$ experiences an initial drop due to the statistical averaging of the two atomic paths, but then it goes back up to unity at steady state. We should mention at this point that the initial state, $|\Psi\rangle_0^{(1)}$, can be generated from vacuum, $|0,0\rangle$, with a probability of 1 by sending one single excited atom through the cavities at $g'\tau'=\pi/4$ and $g''\tau''=\pi/2$ [see Eq. (2.5)].

For an initial state, $|\Psi\rangle_n^{(m)}$, given by Eq. (3.1) for $n\neq 0$ the time evolution of the system is more complicated. Although the condition given by Eq. (3.3) ensures that m is increased by 1 and at the same time n is left unchanged when the lower atomic state is detected, the state vector is not necessarily preserved, as it has been for $n=0$ above when the upper atomic state is detected. This implies that new quantum states exhibiting structures different than the one given by Eq. (3.1) also contribute to the fields, making the trajectory of the system more complicated, and, as the example given by the dotted line in Fig. 6 shows, the purity of the system can be lost at steady state. Here, we start from the initial state, $|\Psi\rangle_1^{(1)}$, and apply $g\tau=\pi/\sqrt{2}$ to satisfy Eq. (3.3). The more complicated trajectory is apparent when comparing the evolution of the field-density matrix depicted in Fig. 5(b) to Figs. 5(a) and 2. The steady state of the fields is not the pure state, $|\Psi\rangle_1^{(6)}$, that we aimed at, although it is close to that. The nonzero field-density matrix elements given by the indices (n_1, m_1, n_2, m_2) are the diagonal terms $(1,1,7,7)$ and $(7,7,1,1)$ equal to 0.500, and the off-diagonal ones $(1,7,7,1)$ and $(7,1,1,7)$ equal to 0.223 (instead of 0.500) that show a mixed quantum state of purity factor

$\xi=0.600$. Considering another interaction parameter of $g\tau=2\pi/\sqrt{2}$ for which the condition of Eq. (3.3) is still satisfied, the effect is even stronger. Only the diagonal elements $(1,1,7,7)$ and $(7,7,1,1)$ survive at steady state having the same value as above 0.500; the off-diagonal elements are equal to -0.01 resulting in the steady-state purity factor $\xi=0.500$. The evolution of $\xi^{(k)}$ as a function of the atom number k is depicted by the dot-dashed line in Fig. 6. Since new quantum states have been involved in the evolution of the system exhibiting different

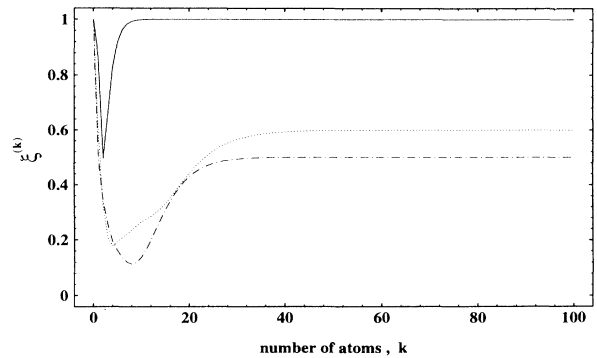


FIG. 6. The evolution of the purity factor $\xi^{(k)}$ as a function of atom number k . The initial states of the fields are the pure states, $|\Psi\rangle_0^{(1)}$, at $g\tau=\pi$ depicted by the solid line, $|\Psi\rangle_1^{(1)}$ at $g\tau=\pi/\sqrt{2}$ depicted by the dotted line, and $|\Psi\rangle_1^{(1)}$ at $g\tau=2\pi/\sqrt{2}$ depicted by the dot-dashed line. The steady state is a coherent superposition, $|\Psi\rangle_0^{(3)}$, of purity factor $\xi=1.0$ in the first case, a mixed state showing some correlation indicated by $\xi=0.6$ in the second case, and a classical mixture of photon numbers 0 and 3 indicated by $\xi=0.5$ in the third case.

structures than the one in Eq. (3.1), the state of the fields irreversibly lost all the correlation and purity. The steady state is a classical (nonlocal) mixture of photon numbers 1 and 7 given by the density operator of the form $|1,7\rangle\langle 1,7| + |7,1\rangle\langle 7,1|$ (apart from a normalization factor).

However, for any initial state of the fields, $|\Psi\rangle_n^{(m)}$, given by Eq. (3.1) one can choose $g\tau$ in such a way that it satisfies the condition given in Eq. (3.3), and at the same time drastically reduces (although does not completely destroy) the probabilities of mixing quantum states of different structures into the evolution of the fields by approximately satisfying Eq. (3.4). In this case, when $g\tau$ is an integer multiple of $\pi/\sqrt{n} + 1$ and *at the same time* it is close to an integer multiple of π/\sqrt{n} , the system does evolve into a steady trapping state that can very well be approximated with the pure entangled trapping state, $|\Psi\rangle_N^{(M)}$. In the example of the initial fields above given by $|\Psi\rangle_1^{(1)}$ we now apply $g\tau = 7\pi/\sqrt{2} = 4.950\pi$. The evolution of the purity of the state of the fields is shown in Fig. 7 by the dot-dashed line and an illustration of the evolution of the field-density matrix is depicted in Fig. 5(c). It is apparent that the system evolves along a trajectory predominantly of state vectors, $|\Psi\rangle_1^{(m)}$, $m=1,2,\dots,6$; new states of different forms have no significant contribution. This is similar to the cases of $n=0$ as can be seen by comparing Fig. 5(c) to 5(a). The steady-state diagonal elements are the same as they were in the examples above for $g\tau = \pi/\sqrt{2}$ and $2\pi/\sqrt{2}$, both $(1,1,7,7)$ and $(7,7,1,1)$ equal to 0.500, while the off-diagonal terms $(1,7,7,1)$ and $(7,1,1,7)$ are now equal to 0.496, resulting in the steady-state purity factor $\xi = 0.992$. The steady state of the system is approximately equal to the entangled trapping state, $|\Psi\rangle_1^{(6)}$. We have found very similar steady states for $g\tau = l\pi/\sqrt{2}$, for $l=7,10,17,\dots$ [within the \pm sign in Eq. (3.1)], although the time evolution can be very different as

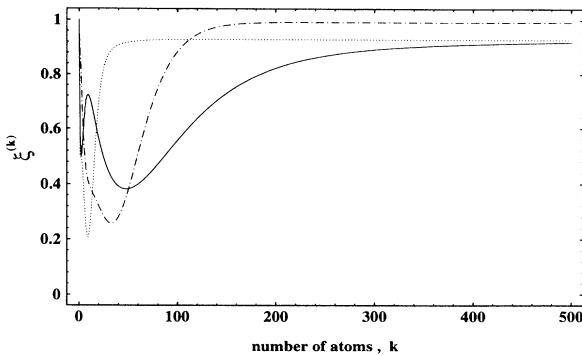


FIG. 7. The evolution of the purity factor $\xi^{(k)}$ as a function of atom number k . The initial state is $|\Psi\rangle_1^{(1)}$ applying $g\tau = l\pi/\sqrt{2}$, where $l=7, 10$, and 17 depicted by the dot-dashed, dotted, and solid lines, respectively. The steady state in each case is approximately the same pure quantum state, $|\Psi\rangle_1^{(6)}$, [within the \pm sign in Eq. (3.1)] although the time evolutions are different. The solid line indicates that in the case of $l=17$ the system is attracted by the pseudotrapping state, $|1,3\rangle - |3,1\rangle$, around $k \approx 9$ which slows down its evolution toward the final state, $|1,7\rangle - |7,1\rangle$ (apart from a normalization factor).

depicted in Fig. 7 by the dot-dashed, dotted, and solid lines, respectively. The evolution of the system toward its steady state is particularly slow, for example, for $l=17$ (solid line), due to its being attracted by the pseudotrapping state, $|1,3\rangle - |3,1\rangle$, along its way around the atom number $k=9$.

The two micromaser fields can be amplified into arbitrary entangled trapping states, $|\Psi\rangle_N^{(M)}$, starting from an appropriate initial state, $|\Psi\rangle_n^{(m)}$, when the interaction parameters $g\tau$ (where $g\tau \equiv g'\tau' = g''\tau''$) approximately satisfy Eqs. (3.3) and (3.4) simultaneously. These two conditions ensure that the fields evolve along statistical mixtures of state vectors of the form given by Eq. (3.1) only. In this case the transient drop in the purity due to the statistical average of the mixture goes back up to 1 as the fields approach the pure trapping state, $|\Psi\rangle_N^{(M)}$. Involving quantum states of different structure into the evolution results in an irreversible loss of purity, and the system evolves into a mixed quantum state of reduced or vanishing correlation. The same occurs in the case of unequal interaction parameters as we mentioned earlier. Although new structures will not appear when $g'\tau'$ is different than $g''\tau''$ [both approximately satisfying Eqs. (3.3) and (3.4)] the fields will not be amplified symmetrically, resulting in a reduction of correlation at steady state. In the example of the initial state, $|\Psi\rangle_1^{(1)}$, above, applying $g'\tau'$ and $g''\tau''$ equal to $l\pi/\sqrt{2}$ ($l=7,10,17$) and now using different l 's for the different cavities, the correlation is completely gone and the purity factor is $\xi = 0.5$ at steady state.

C. Preparation of the initial state, $|\Psi\rangle_n^{(1)}$, and switching to its amplification

For $n \neq 0$ the preparation of the fields in the appropriate initial state, $|\Psi\rangle_n^{(1)}$, starting from the number state, $|n,n\rangle$, is not as simple as it has been for $n=0$ above (on the production of number states, see Refs. [9,12,18]). The reason for this is similar to the one in the amplifying step of the procedure above when contrasting the two cases of $n=0$ and $n \neq 0$, namely, undesirable quantum states show up when the atom leaves the interaction in its upper state. Although the probability of this effect cannot in principle be destroyed completely, it can be drastically reduced by applying the same idea as above. Let us send one single excited atom through the fields started from the number state, $|n,n\rangle$, and set the interaction parameters, $g'\tau'$ and $g''\tau''$, in the two cavities as follows ($g'\tau' = g''\tau''$ is required only in the amplifying procedure, not here). First of all, $g'\tau'$ must satisfy the condition $|C'_{n+1}| = |S'_{n+1}|$. On the other hand, we need the second interaction parameter, $g''\tau''$, to approximately satisfy conditions $|S''_{n+1}| \approx 1$ and $S''_n \approx 0$ *simultaneously*. In this case Eq. (2.5) tells us that the probability of detecting the outgoing atom in its upper state is close to zero, while the other atomic path provides us with fields in a state approximately equal to $|\Psi\rangle_n^{(1)}$. We have seen above that this obviously works for a vacuum, $n=0$. In the case of $n=1$, choosing, for example, $g'\tau' = \pi/(4\sqrt{2})$ and $g''\tau'' = 17\pi/(2\sqrt{2}) = 6.01\pi$ gives us the probability of

0.1% to detect the upper atomic state and the general fields can very well be approximated by the pure state, $|\Psi\rangle_1^{(1)}$. Once the initial state, $|\Psi\rangle_n^{(1)}$, is prepared for amplification by one single atom we can proceed to the second (amplifying) step of the procedure by switching the interaction parameters to the appropriate values discussed above.

The switching itself sounds simple in principle, but it raises some technical difficulties in a real experiment. It is easy to see that, in general, one cannot match the interaction parameters between the two steps (preparation of the state and its amplification) by simply switching the velocity of the atomic beam. In order to do that the ratio, $g'\tau'/g''\tau''$, would need to remain the same throughout the procedure. This, however, is not possible because the equality condition, $g'\tau'=g''\tau''$, of the second step cannot possibly be met in the first one (see the conditions above). Since the purpose of this condition is to assure a symmetric amplification, it can be ignored only if a trapping state of first-order correlation ($m=1$) is to be produced (since there is no amplification here at all). In this case one can find interaction parameters, $g'\tau'\neq g''\tau''$, that prepare the state, $|\Psi\rangle_n^{(1)}$, starting from the number state, $|n, n\rangle$, in the first step and then trap it by simply switching the atomic velocity in the second one. This obviously imposes a restriction on the set of parameters that have been found above for the two steps separately, since now we need only those of them that satisfy the conditions of both steps simultaneously. For example, the conditions to generate $|\Psi\rangle_0^{(1)}$ from $|0, 0\rangle$ are $g'\tau'=\pi/4+k\pi/2$ and $g''\tau''=\pi/2+l\pi$, while those to trap this state are $g'\tau'=p\pi$ and $g''\tau''=q\pi/\sqrt{2}$. Choosing the integers k, l, p , and q to be 2, 8, 5, and 48, respectively, the ratio $g'\tau'/g''\tau''$ is 5/34 in both steps. Thus, a simple change in the atomic velocity (in this example a decrease by a factor of 4) after the first atom will trap the fields in the state $|\Psi\rangle_0^{(1)}$. We should mention at this point that, as is going to be shown in the next section (also see Ref. [14]), the smaller the correlation (m) the longer the lifetime of the pure state is at the presence of dissipations (see also in Ref. [14]). Therefore a simple procedure to generate the long-lived state, $|\Psi\rangle_n^{(1)}$, from the number state, $|n, n\rangle$, is possible. This nonlocal entanglement, as discussed in Ref. [19], can prove useful in several interesting applications, such as to generate interatomic Einstein-Podolsky-Rosen (EPR) correlations between spatially distinct atomic beams that can, for example, be applied to test the principle of complementarity of quantum mechanics.

The generation of higher-order correlations, however, seems to be more complicated. Since the equality condition, $g'\tau'=g''\tau''$, is crucial for pure amplification, such parameters that can be switched by atomic velocities cannot be found. A rather unrealistic adjustment of the cavity lengths or of the coupling constants relative between the two cavities seems to be necessary when proceeding from the preparation to the amplification step. There may be some, probably difficult, technical tricks to get around this problem, for example, shooting the single atom in the first step through the cavities at an angle allowing for a control of the individual interaction times in

either of the two cavities separately.

Another possibility to reconcile the two steps of the procedure may be to use conditional measurements in the first step [12]. The two possible outcomes when detecting the final state of the first single atom imply two possible pure states for the fields. We can set the parameters in such a way that one of these would be the desired $|\Psi\rangle_n^{(1)}$ for the fields. Thus, we impose the condition that the atomic state generating $|\Psi\rangle_n^{(1)}$ needs to be detected in order to proceed to the amplifying step of the procedure. Starting, for example, from the field state, $|1, 1\rangle$, and using $g'\tau'=g''\tau''=7\pi/4\sqrt{2}$ the detection of the lower atomic state, $|b\rangle$, (the probability of which is about 50% in this example) ensures that the field state, $|\Psi\rangle_1^{(1)}$, has been generated. (If we detect $|a\rangle$ then we need to reconstruct $|1, 1\rangle$ and start again until $|b\rangle$ is detected.) Now lowering the atomic velocity by a factor of 4 we are back to the same amplifying step as the one discussed in Sec. IIIB above in detail to generate the trapping state, $|\Psi\rangle_0^{(6)}$.

We have shown in this section that entangled trapping states, $|\Psi\rangle_N^{(M)}$, given by Eq. (3.1) of arbitrary N and M can be produced using a two-step procedure that is based on conditions regarding the interaction parameters of the two cavities. In principle, N and M can be made arbitrarily large, resulting in a nonlocal quantum superposition of distinct macroscopical fields—sometimes referred to as a nonlocal Schrödinger cat. Since quantum superpositions are well known to be very sensitive to dissipations [14] we are going to study the effect of cavity losses and finite temperature on the method discussed above in the next section.

IV. THE EFFECT OF DISSIPATION ON THE PRODUCTION OF ENTANGLED TRAPPING STATES

Pure steady-state entanglement of the nonlocal micromaser fields has been found in the absence of dissipation in the form of trapping states, $|\Psi\rangle_N^{(M)}$, given by Eq. (3.1). In this section we study the effect of finite losses and temperature numerically, concentrating on the production of these states. We assume that the interaction time an atom spends in the cavities is much shorter than the cavity lifetime. (In a typical experimental setup the difference is three orders of magnitude.) In this case we can ignore the decay of the fields during the time an atom is inside the cavities and separate the evolution of the system into two parts: atom-field interaction (pumping) and decay of the fields (damping). Thus, the field-density matrix at the instant when an atom leaves cavity 2 can be calculated from Eq. (2.2), resulting in the matrix $\rho(0)$, the decay of which is then calculated from this initial condition as a function of time by applying the solution of the standard master equation for a field mode of an empty cavity damped to a reservoir of finite temperature given by

$$\rho_n^{\{k\}}(t) = e^{-\gamma(k/2)t} \sum_{l=0}^n \sum_{m=n-l}^{\infty} C_{n,m,l}^{\{k\}} \frac{A^m}{B^{m+k+1}} \left[\frac{A'}{A} \right]^{n-l} \times \left[\frac{B'}{B} \right]^l \rho_m^{\{k\}}(0). \quad (4.1)$$

Here, $\rho_n^{\{k\}} \equiv \rho_{nm}$ with $k = m - n$, γ is the cavity decay rate, and t is time. The coefficients are given by

$$C_{n,m,l}^{\{k\}} \equiv (-1)^l \binom{m+k+l}{l} \binom{m}{n-l} \times \left[\binom{m+k}{n+k} / \binom{m}{n} \right]^{1/2}, \quad (4.2)$$

$A \equiv (n_b + 1)(1 - e^{-\gamma t})$, $B \equiv 1 + n_b(1 - e^{-\gamma t})$, $A' \equiv e^{-\gamma t} - n_b(1 - e^{-\gamma t})$, and $B' \equiv A' - e^{-\gamma t}$, where n_b is the average number of thermal photons. A derivation of this solution is given in the Appendix (see also Ref. [17]). It is easy to show that in the special case of zero temperature, i.e., $n_b = 0$, Eq. (4.1) reduces to

$$\rho_n^{\{k\}}(t) = e^{-\gamma(n+k/2)t} \sum_{m=0}^{\infty} \left[\binom{m+k}{n+k} \binom{m}{n} \right]^{1/2} \times (1 - e^{-\gamma t})^m n^{-n} \rho_m^{\{k\}}(0). \quad (4.3)$$

The two fields decay according to this time-dependent density matrix during the time interval until the next atom arrives. Hence, the time evolution of the fields for a stream of atoms is calculated by numerically iterating the two cycles of pumping and damping by applying Eqs. (2.2) and (4.1), respectively. Apparently, the pump statistics of the micromasers can also be taken into account via the distribution of time intervals of the decay cycles in the procedure. The effect of pump fluctuations will be studied later on by assuming Poissonian statistics for the atomic beam.

In the first examples we consider regular pump statistics and the temperature of the reservoir is assumed to be zero [Eq. (4.3) is applied]. We study the effect of cavity losses on the production of entangled trapping states discussed in the earlier sections. Let us start the fields from a pure state, $|\Psi\rangle_0^{(1)}$, and apply $g\tau = \pi$. Figure 8 shows the evolution of the purity factor $\xi^{(k)}$ for four different values of γt , illustrating the evolution of the fields. We find that provided the losses are not too large (in this example if $\gamma t \leq 0.001$) the same entangled trapping state, $|\Psi\rangle_0^{(3)}$, is produced in the short-time transient regime as in the absence of losses, followed by a decay of the correlation the rate of which depends on γt (see solid and dot-dashed lines in Fig. 8). For larger losses the complete entanglement has no chance to build up (dashed and dotted lines). Some correlation can be found for $\gamma t = 0.01$ at short times (dashed line), but no correlation at all for $\gamma t = 0.1$ (dotted line). The steady state of the fields in each of these four cases is a mixed quantum state of no off-diagonal elements in the density matrix, i.e., no correlation between the fields. The photon statistics are depicted in Fig. 9(a), and apparently the steady state is a (nonlocal) classical superposition of the photon numbers 0 and 3 if $\gamma t \leq 0.001$. The only nonzero matrix elements are the (0,0,3,3) and (3,3,0,0) equal to 0.5 resulting in a purity factor of $\xi = 0.5$ (see solid and dot-dashed lines Fig. 8). On the other hand, Fig. 9(a) shows how this classical superposition decays due to losses exceeding this threshold ($\gamma t > 0.001$) until finally the fields settle down

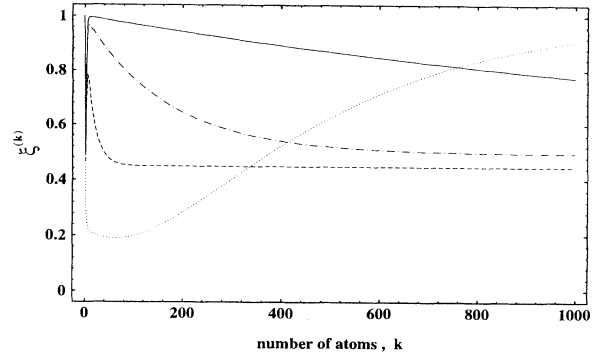


FIG. 8. The evolution of the purity factor $\xi^{(k)}$ as a function of atom number k for four different cavity losses of $\gamma t = 0.0001$, 0.001, 0.01, and 0.1 depicted by solid, dot-dashed, dashed, and dotted lines, respectively. The initial state of the fields is the pure state $|\Psi\rangle_0^{(1)}$, applying $g\tau = \pi$, which would evolve into the steady state $|\Psi\rangle_0^{(3)}$ in the absence of losses. Apparently, in the cases of small losses (solid and dot-dashed lines) this state can build up in the transient regime where $\xi^{(k)}$ is close to 1 and then decay into the classical superposition of the above photon numbers 0 and 3. In the case of large losses (dotted line) there is no transient correlation and the steady state spreads out toward the vacuum of $\xi = 1.0$.

to the vacuum (of steady-state purity factor $\xi = 1.0$, the dotted line in Fig. 8). These two regimes of small and large losses can also be distinguished in the next example where the fields are started from the initial state, $|\Psi\rangle_1^{(1)}$, and $g\tau = 7\pi/\sqrt{2}$ is applied. The evolution of the purity factor $\xi^{(k)}$ is depicted in Fig. 10 for the same four values of γt as in Fig. 8. It can be seen that some correlation builds up in the transient regime if $\gamma t \leq 0.001$ (see solid and dot-dashed lines in Fig. 10) while there is no correlation between the fields at any time if the losses are larger. Comparing Fig. 10 to Fig. 8 it is apparent that the quantum superposition, $|\Psi\rangle_1^{(6)}$, that we want to generate in the present example is more sensitive to cavity losses than the one $|\Psi\rangle_0^{(3)}$ was before, and the threshold for a correlation to build up is higher. This has been discussed by others, for example, in Ref. [14]: that a quantum superposition decays exponentially faster for superposed states of larger separation (or order of correlation, which is M in our case). The steady-state photon statistics of the fields for the present example is depicted in Fig. 9(b) showing a nonlocal classical superposition of photon numbers 1 and 7 for small losses ($\gamma t < 0.001$) that spreads out toward the vacuum if the losses are larger.

We also studied the (zero temperature) decay of the entanglement in the two examples of the quantum states above for Poissonian pump statistics. Comparing Fig. 11 to Figs. 8 and 10 it can be seen that apart from the fluctuations there is no significant difference in the decay of the correlation between the regular and Poissonian cases. For small cavity losses where the average of γt is smaller than 0.01 even the fluctuations are negligible. This suggests that the transient production of entanglement is not significantly sensitive to pumping fluctuations.

Now, let us assume that finite thermal radiation is present in the cavities [Eq. (4.1) is applied], and consider regular pump statistics. The most significant effect is that a coupling arises between the blocks in the photon number space that were disconnected by the trapping states at zero temperature. As a result of this new diagonal elements contribute to the density matrix, located exactly at the trapping points of the adjacent blocks, although new correlation obviously does not build up. The photon statistics of the fields starting from the state $|\Psi\rangle_0^{(1)}$ and applying $g\tau=\pi$ are depicted in Fig. 12 for four different mean numbers of thermal photons at a cavity loss of $\gamma t=0.0001$, showing the new terms arising at the adjacent trapping points of the system. The larger the temperature the more diagonal trapping points are populated besides the zero-temperature ones, (0,0,3,3) and (3,3,0,0). Another significant effect of thermal radiation is the enhancement of the decay of correlation between the micromasers. The off-diagonal terms of the field-density

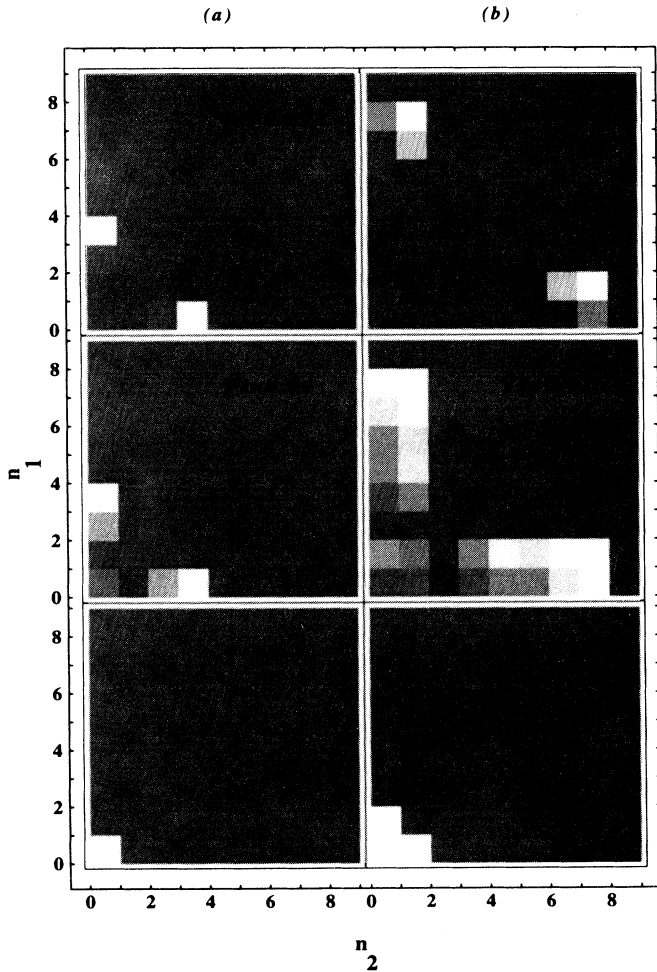


FIG. 9. Steady-state photon statistics of the fields started from the initial pure states (a) $|\Psi\rangle_0^{(1)}$, at $g\tau=\pi$ and (b) $|\Psi\rangle_1^{(1)}$, at $g\tau=7\pi/\sqrt{2}$ for three different losses of $\gamma t=0.001$, 0.01, and 0.1 given in the figure. In the case of small cavity losses the steady states of the fields are classical mixtures of the photon numbers (a) 0 and 3 and (b) 1 and 7, which spread out toward the vacuum for increasing losses.

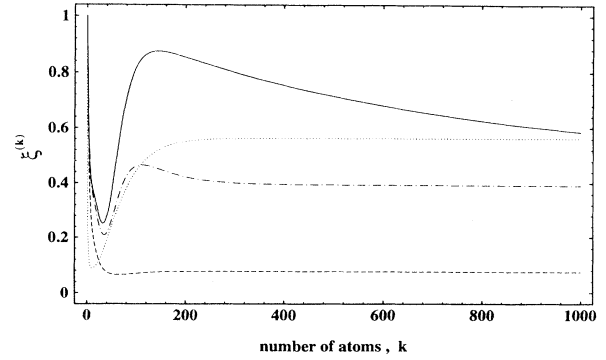


FIG. 10. The evolution of the purity factor $\xi^{(k)}$ as a function of atom number k for four different cavity losses of $\gamma t=0.0001$, 0.001, 0.01, and 0.1 depicted by solid, dot-dashed, dashed, and dotted lines, respectively. The initial state of the fields is the pure state, $|\Psi\rangle_1^{(1)}$, applying $g\tau=7\pi/\sqrt{2}$, which would evolve into the steady state, $|\Psi\rangle_1^{(6)}$, in the absence of losses. It can be seen that the losses are large enough to prevent this state from building up at any time, although some correlation arises in the case of the smallest amount of loss (solid line).

matrix decay faster for larger numbers of thermal photons. As an example, Fig. 13 depicts the evolution of the purity factor $\xi^{(k)}$ toward the state of the fields described in Fig. 12, showing the enhanced decay of correlation for the same four mean numbers of thermal photons and cavity loss. Comparing Fig. 13 to Fig. 8 it is apparent that for small temperatures ($n_b < 0.01$) the short-time transient entanglement can still be produced. In fact, finite temperature seems to predominantly affect the steady state rather than the transient regime.

Assuming the experimentally available lowest temperature 0.1 K and the corresponding mean thermal photon

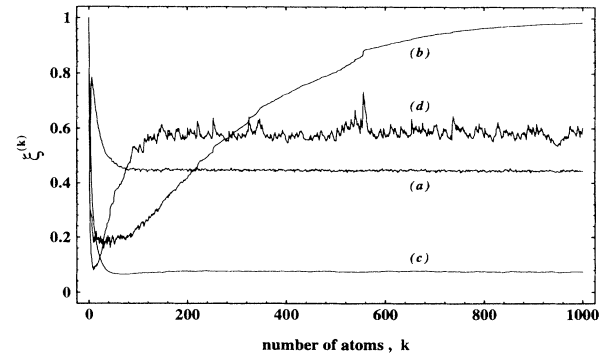


FIG. 11. The evolution of the purity factor $\xi^{(k)}$ as a function of atom number k for Poissonian pump statistics. The initial state of the fields is for curves a and b $|\Psi\rangle_0^{(1)}$ at $g\tau=\pi$ and for curves c and d $|\Psi\rangle_1^{(1)}$ at $g\tau=7\pi/\sqrt{2}$. The average loss is curves a and c $\gamma t=0.01$ and curves b and d $\gamma t=0.1$. Considering Figs. 8 and 10 we find that apart from the fluctuations the short-time transient behavior is not significantly affected as compared to regular pump statistics. For smaller cavity losses, γt , even the fluctuations are negligible.

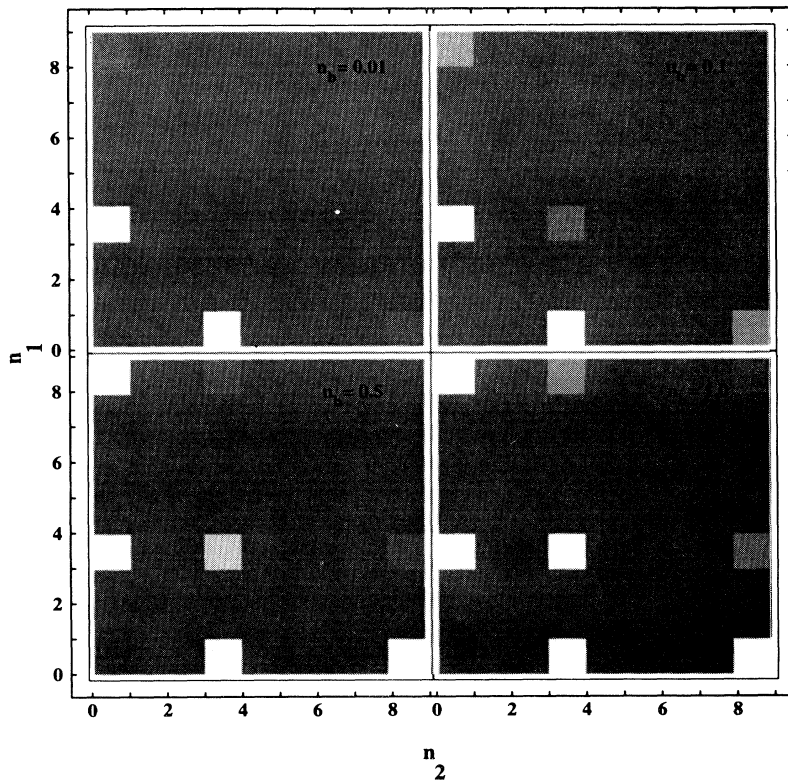


FIG. 12. Density plot of the photon statistics for four different values of the mean thermal photon number n_b that are given in the figure at cavity loss of $\gamma t = 0.0001$ and at atom number $k = 1000$. The initial state of the fields is the pure state, $|\Psi\rangle_0^{(1)}$, applying $g\tau = \pi$, the steady state of which would be $|\Psi\rangle_0^{(3)}$ in the absence of losses. New trapping states contribute due to the coupling between the blocks that were disconnected at zero temperature.

number $n_b = 3 \times 10^{-5}$, it is easy to see that in the case of $\gamma t = 0.001$ the effect of thermal radiation can be neglected. If the cavity lifetime were assumed to be $1/\gamma = 1.0$ s then according to Fig. 14 the entangled state, $|\Psi\rangle_0^{(3)}$, survives with purity factors of $\xi \cong 90\%$, 80% , and 70% for time intervals of about 30, 80, and 150 ms, respectively. Introducing the generally used pumping parameters N_{ex} , and θ , where $N_{\text{ex}} = 1/\gamma t$ and $\theta = g\tau\sqrt{N_{\text{ex}}}$, the above pumping corresponds to $N_{\text{ex}} = 1000$ and $\theta = \pi\sqrt{N_{\text{ex}}} = 99.3$ (since $g\tau = \pi$ is required by the ampli-

fying mechanism to generate the state $|\Psi\rangle_0^{(3)}$). The above comparison of regular and Poissonian pumping statistics suggests that this estimate is not particularly sensitive to pump fluctuations. It is also in accordance with the two usual “micromaser conditions.” First, assuming the experimentally available coupling $g \cong 40$ kHz the separation to pumping and damping cycles is well justified since $\tau \ll 1/\gamma$. On the other hand, it follows from $\gamma t = 0.001$ ($N_{\text{ex}} = 1000$) that the time interval between the successive atoms (or the average of it for Poissonian statistics) is

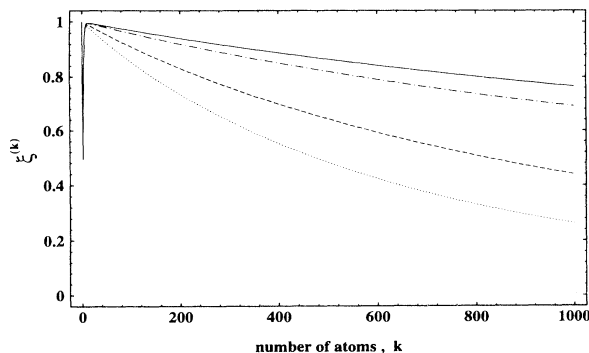


FIG. 13. The evolution of the purity factor $\xi^{(k)}$ as a function of atom number k for four different mean numbers of thermal photons $n_b = 0.01, 0.1, 0.5,$ and 1.0 depicted by solid, dot-dashed, dashed, and dotted lines, respectively, at a cavity loss of $\gamma t = 0.0001$. The initial state of the fields is the pure state, $|\Psi\rangle_0^{(1)}$, applying $g\tau = \pi$, the steady state of which would be $|\Psi\rangle_0^{(3)}$ in the absence of losses.

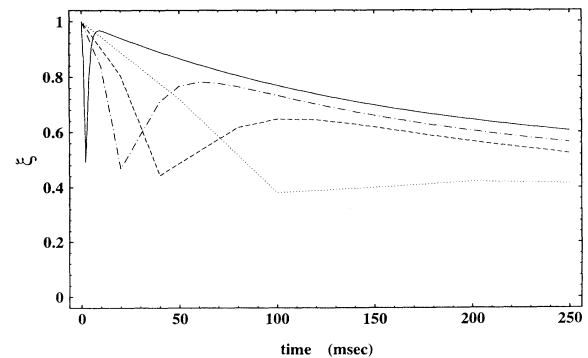


FIG. 14. Time evolution of the purity factor ξ for $N_{\text{ex}} = 1000, 100, 50,$ and 20 depicted by solid, dot-dashed, dashed, and dotted lines, respectively, when starting from the initial state, $|\Psi\rangle_0^{(1)}$, applying $g\tau = \pi$. Transient correlation starts building up when N_{ex} exceeds 50 that grows up to a complete (transient) entanglement into the state, $|\Psi\rangle_0^{(3)}$, above $N_{\text{ex}} = 1000$.

about $t \cong 1.0$ ms, which implies that there is at most one atom in the cavities at a time because $\tau \ll t$. Going for lower values of γt (larger N_{ex}) in order to hold the entanglement for a longer time interval, or to be able to deal with a superposition of larger separation (or order of correlation) M , we need to elongate the cavity lifetime. The time interval t between the atoms could be reduced only if g were enlarged to have the second micromaser condition satisfied.

As a summary to this section it can be said that, although finite dissipation prevents the steady-state production of entangled nonlocal fields, transient correlation insensitive to thermal radiation and pumping fluctuations can still build up for a pumping, N_{ex} , that exceeds a certain threshold established by the losses. This suggests that the state of the fields undergoes a transition from an uncorrelated to a correlated behavior above threshold. The lifetime of the correlated regime depends on the cavity damping rate γ and the separation (or order of correlation) M of the two trapped number states in the quantum superposition. Experimental realization of transient entanglement of nonlocal fields employing two-field trapping states of small photon numbers seems to be feasible by the presently available exceedingly high- Q ($Q \cong 10^{10}$) micromaser cavities at low temperatures ($T=0.1$ K, $n_b = 3 \times 10^{-5}$), and could be extended to macroscopical quantum superpositions by using longer cavity lifetimes and stronger atom-field coupling in the near future.

V. SUMMARY

In the present paper the fields of two coupled micromasers are studied. The state of the atoms establishing the coupling via passing through the cavity 1 first and then cavity 2 is nonselectively measured after the interaction (see Fig. 1). In the absence of dissipation the possible steady states are the various superpositions of two-field trapping number states satisfying the trapping condition given by Eq. (2.3), many of which are pure quantum states given by Eq. (2.12). They rely on the fact that the photon number space consists of disconnected blocks in this case of two dimensions due to the two nonlocal fields and each block may contribute to the superposition with its own trapping number state. The realization of one of these steady states, i.e., populating a certain configuration of trapping numbers, depends upon the initial state of the fields and the interaction parameters of the micromasers. The time evolution of the fields toward these steady states is studied numerically, concentrating mainly on the production of pure entangled states of the form $|N, N+M\rangle \pm |N+M, N\rangle$. Here, N and $N+M$ are arbitrary trapping numbers belonging to disconnected blocks of the photon number space, and M specifies the order of correlation between the two nonlocal fields. They, in principle, can be made arbitrarily large resulting in a steady-state nonlocal quantum superposition of distinct macroscopical fields—sometimes referred to as a nonlocal Schrödinger cat. Starting from a number state, $|N, N\rangle$, these states can be produced using a two-step procedure. First, we introduce some correlation into the system via generating the above state of $M=1$ by one

single atom and then amplify it to a larger M corresponding to the trapping state above. Both steps are based on special conditions regarding the interaction parameters, $g't'$ and $g''t''$, of the two cavities. They are chosen to ensure that the fields evolve along statistical mixtures of state vectors of the form given by Eq. (3.1) only. In this case the purity of the fields after experiencing a transient drop due to the statistical mixture will be regained at steady state showing a pure quantum state of the structure above. An inclusion of different quantum states into the evolution, or an asymmetrical amplification of the state vector (when $g't' \neq g''t''$) would result in an irreversible loss of purity and mixed quantum states of no correlation at steady state. In the absence of losses this procedure provides us with arbitrary (micro- as well as macroscopical) quantum superpositions of nonlocal fields at steady state.

Introducing dissipation into the system by applying our solution of the standard master equation of a damped harmonic oscillator we find that although entanglement in the above form cannot be produced at steady state it can build up in the short-time transient regime if the losses are small enough. The rate of the decay of correlation depends upon the cavity lifetime and the separation (or order of correlation) M of the photon numbers in the superposition above. On the other hand, for exceedingly large losses correlation has no chance to arise at any time. The system undergoes a transition from an uncorrelated to a correlated behavior when the pumping parametrized by N_{ex} exceeds a certain threshold between the large- and small-loss regimes ($g\tau$ is fixed throughout the procedure). In the small-loss (large N_{ex}) regime the entanglement finally decays into a classical mixture of the above photon numbers, N and $N+M$, at steady state while in the large-loss (small N_{ex}) regime the photon statistics spreads out toward a vacuum. It is also shown that the transient behavior is only slightly modified by finite temperature and pump fluctuations. Finite temperature enhances the decay rate, mainly affecting the steady state of the fields, and at the same time establishes a coupling between the disconnected blocks of the photon space allowing for new but only diagonal trapping states to contribute. We conclude that an entanglement of nonlocal micromaser fields can be produced via this nonselective measurement scheme by utilizing the two-field trapping states and the discussed amplification mechanism—in principle, even on the macroscopic level. Experimental realization of these states seems to be feasible in the transient regime by the presently available facilities for trapping states of microscopically small photon numbers, and could be extended to macroscopical quantum superpositions—nonlocal Schrödinger cats—by applying longer cavity lifetimes and stronger atom-field coupling in the near future.

ACKNOWLEDGMENTS

This research was supported by a grant from the Office of Naval Research, Grant No. N00014-92-J-1233, by a grant from the National Science Foundation, Grant No. PHY-9201912, and by a grant from the PSC-CUNY Research Award Program.

APPENDIX

In Sec. IV the effect of finite losses and temperature in the two micromaser cavities is studied by applying the time-dependent density matrix given by Eq. (4.1). We show here that it is the solution of the standard interaction-picture master equation for a field mode of an empty cavity coupled to a reservoir of finite temperature that reads as

$$\dot{\rho} = \frac{\gamma}{2} [(n_b + 1)(2a\rho a^\dagger - a^\dagger a \rho - \rho a^\dagger a) + n_b(2a^\dagger \rho a - a a^\dagger \rho - \rho a a^\dagger)], \quad (\text{A1})$$

where γ is the coupling constant between the cavity mode and the reservoir, a^\dagger and a are the mode creation and annihilation operators, and n_b is the average number of thermal photons [17]. It can be seen in the number representation that the elements of the density matrix ρ_{nm} are coupled only along the same diagonal. Introducing $\rho_n^{[k]} \equiv \rho_{nm}$, where $k = m - n$, the master equation reads as

$$\begin{aligned} \dot{\rho}_n^{[k]} = & \gamma(n_b + 1) \left[\sqrt{(n+1)(n+k+1)} \rho_{n+1}^{[k]} \right. \\ & \left. - \left[n + \frac{k}{2} \right] \rho_n^{[k]} \right] \\ & + \gamma n_b \left[\sqrt{n(n+k)} \rho_{n-1}^{[k]} - \left[n + 1 + \frac{k}{2} \right] \rho_n^{[k]} \right]. \end{aligned} \quad (\text{A2})$$

Defining the function

$$g^{[k]}(z, t) \equiv \sum_{n=0}^{\infty} \rho_n^{[k]}(t) \left[\frac{(n+k)!}{n!} \right]^{1/2} z^n, \quad (\text{A3})$$

the master equation Eq. (A2) can be transformed into a partial differential equation for $g^{[k]}(z, t)$ given by

$$\frac{\partial g^{[k]}}{\partial t} + (z-1)[1-n_b(z-1)] \frac{\partial g^{[k]}}{\partial z} = \left[n_b(z-1)(k+1) - \frac{k}{2} \right] g^{[k]}, \quad (\text{A4})$$

the solution of which reads as

$$g^{[k]}(z, t) = e^{-\gamma(k/2)t} \sum_{n=0}^{\infty} \rho_n^{[k]}(0) \left[\frac{(n+k)!}{n!} \right]^{1/2} \frac{A^n}{B^{n+k+1}}, \quad (\text{A5})$$

where

$$A \equiv 1 - (z-1)[n_b(1-e^{-\gamma t}) - e^{-\gamma t}], \quad (\text{A6})$$

$$B \equiv 1 - n_b(z-1)(1-e^{-\gamma t}). \quad (\text{A7})$$

The inverse transformation of Eq. (A3) is given by

$$\rho_n^{[k]}(t) = \frac{1}{\sqrt{n!(n+k)!}} \left. \frac{\partial^n g^{[k]}}{\partial z^n} \right|_{z=0}, \quad (\text{A8})$$

resulting in the final solution for the density matrix

$$\rho_n^{[k]}(t) = e^{-\gamma(k/2)t} \sum_{l=0}^n \sum_{m=n-l}^{\infty} C_{n,m,l}^{[k]} \left[\frac{A^m}{B^{m+k+1}} \left(\frac{A'}{A} \right)^{n-l} \left(\frac{B'}{B} \right)^l \right]_{z=0} \rho_m^{[k]}(0), \quad (\text{A9})$$

where

$$C_{n,m,l}^{[k]} \equiv (-1)^l \binom{m+k+l}{l} \binom{m}{n-l} \left[\frac{\binom{m+k}{n+k}}{\binom{m}{n}} \right]^{1/2}, \quad (\text{A10})$$

and $A' \equiv \partial A / \partial z$, $B' \equiv \partial B / \partial z$. It is easy to show that in the special case of zero temperature this reduces to

$$\rho_n^{[k]}(t) = e^{-\gamma(n+k/2)t} \sum_{m=0}^{\infty} \left[\frac{\binom{m+k}{n+k}}{\binom{m}{n}} \right]^{1/2} (1-e^{-\gamma t})^{m-n} \rho_m^{[k]}(0). \quad (\text{A11})$$

[1] Generation of macroscopic superpositions in a micromaser via tangent and cotangent states was suggested by P. Filipowicz, J. Javanainen, and P. Meystre, *J. Opt. Soc. Am. B* **3**, 906 (1986); J. J. Slosser, P. Meystre, and S. L. Braunstein, *Phys. Rev. Lett.* **63**, 934 (1989); J. J. Slosser and P. Meystre, *Phys. Rev. A* **41**, 3867 (1990); J. J. Slosser, P. Meystre, and E. M. Wright, *Opt. Lett.* **15**, 233 (1990); P. Meystre, J. Slosser, and M. Wilkens, *Phys. Rev. A* **43**, 4959 (1991).

[2] For a recent review, see H. Walther, *Phys. Rep.* **219**, 201 (1992); also H. Walther, *Phys. Scr.* **T23**, 165 (1988); F. Diedrich, J. Krause, G. Rempe, M. O. Scully, and H. Walther, *IEEE J. Quantum Electron.* **QE-24**, 1314 (1988).

[3] For the quantum theory of the micromaser, see P. Filipowicz, J. Javanainen, and P. Meystre, *Phys. Rev. A* **34**, 3077 (1986); the semiclassical theory is given by A. M. Guzman, P. Meystre, and E. W. Wright, *ibid.* **40**, 2471 (1989).

- [4] L. A. Lugiato, M. O. Scully, and H. Walther, *Phys. Rev. A* **36**, 740 (1987).
- [5] The first masing in a single-atom micromaser was reported by D. Meschede, H. Walther, and G. Müller, *Phys. Rev. Lett.* **54**, 551 (1985); G. Rempe, F. Schmidt-Kaler, and H. Walther, *ibid.* **64**, 2783 (1990).
- [6] Super-radiance in a micromaser cavity was first reported by J. M. Raimond, P. Goy, M. Gross, C. Fabre, and S. Haroche, *Phys. Rev. Lett.* **49**, 1924 (1982); on the two-photon micromaser, see M. Brune, J. M. Raimond, P. Goy, L. Davidovich, and S. Haroche, *ibid.* **59**, 1899 (1987); and L. Davidovich, J. M. Raimond, M. Brune, and S. Haroche, *Phys. Rev. A* **36**, 3771 (1987).
- [7] E. T. Jaynes and F. W. Cummings, *Proc. IEEE* **51**, 89 (1963); H. Paul, *Ann. Phys. (Leipzig)* **11**, 411 (1963); J. H. Eberly, N. B. Narozhny, and J. J. Sanchez-Mondragon, *Phys. Rev. Lett.* **23**, 44 (1980); the experimental proof of the quantum collapse and revival predicted by the Jaynes-Cummings model was reported by G. Rempe, H. Walther, and N. Klein, *ibid.* **58**, 353 (1987).
- [8] Quantum island states have recently been found in the micromaser by P. Bogár, J. A. Bergou, and M. Hillery, *Phys. Rev. A* **50**, 754 (1994); P. Bogár and J. A. Bergou (unpublished).
- [9] J. Krause, M. O. Scully, and H. Walther, *Phys. Rev. A* **36**, 4547 (1987); P. Meystre, *Opt. Lett.* **12**, 668 (1987); in *Squeezed and Nonclassical Light*, edited by P. Tombesi and E. R. Pike (Plenum, New York, 1988); H. Paul, *J. Mod. Opt.* **36**, 515 (1989); F. W. Cummings and A. K. Rajagopal, *Phys. Rev. A* **39**, 3414 (1989).
- [10] P. Meystre, G. Rempe, and H. Walther, *Opt. Lett.* **13**, 1078 (1988).
- [11] For the linear theory of this system, see J. A. Bergou and M. Hillery, *Phys. Rev. A* **44**, 7502 (1991).
- [12] The same system with conditional measurements of atoms is studied by P. Bogár, J. A. Bergou, and M. Hillery, *Phys. Rev. A* (to be published).
- [13] Nonlocal microwave-field quantum states have been found in a similar system by L. Davidovich, A. Maali, M. Brune, J. M. Raimond, and S. Haroche, *Phys. Rev. Lett.* **71**, 2360 (1993).
- [14] A. O. Caldeira and A. J. Leggett, *Phys. Rev. A* **31**, 1059 (1985); D. F. Walls and G. J. Milburn, *ibid.* **31**, 2403 (1985); C. M. Savage and D. F. Walls, *ibid.* **32**, 2316 (1985).
- [15] E. B. Davies, *Quantum Theory of Open Systems* (Academic, London, 1976); K. Krauss, *States, Effects and Operations: Fundamental Notions of Quantum Theory* (Springer-Verlag, Berlin, 1983).
- [16] The nonlinear theory and numerical simulations of this system at significant losses are given by P. Bogár, J. A. Bergou, and M. Hillery (unpublished).
- [17] The problem has been studied in great detail, for example, in W. H. Louisell, *Quantum Statistical Properties of Radiation* (Wiley, New York, 1973); H. Haken, *Laser Theory* (Springer-Verlag, Berlin, 1970); for a recent solution, see also A. Mufti, H. A. Scmitt, A. B. Balantekin, and M. Sargent III, *J. Opt. Soc. Am. B* **10**, 2100 (1993).
- [18] M. Brune, S. Haroche, V. Lefevre, J. M. Raimond, and N. Zagury, *Phys. Rev. Lett.* **65**, 976 (1990); M. Brune, S. Haroche, J. M. Raimond, L. Davidovich, and N. Zagury, *Phys. Rev. A* **45**, 5193 (1992).
- [19] Entangled trapping states of nonlocal fields are applied to generate correlations between two spatially separated atomic beams in P. Bogár and J. A. Bergou (unpublished).

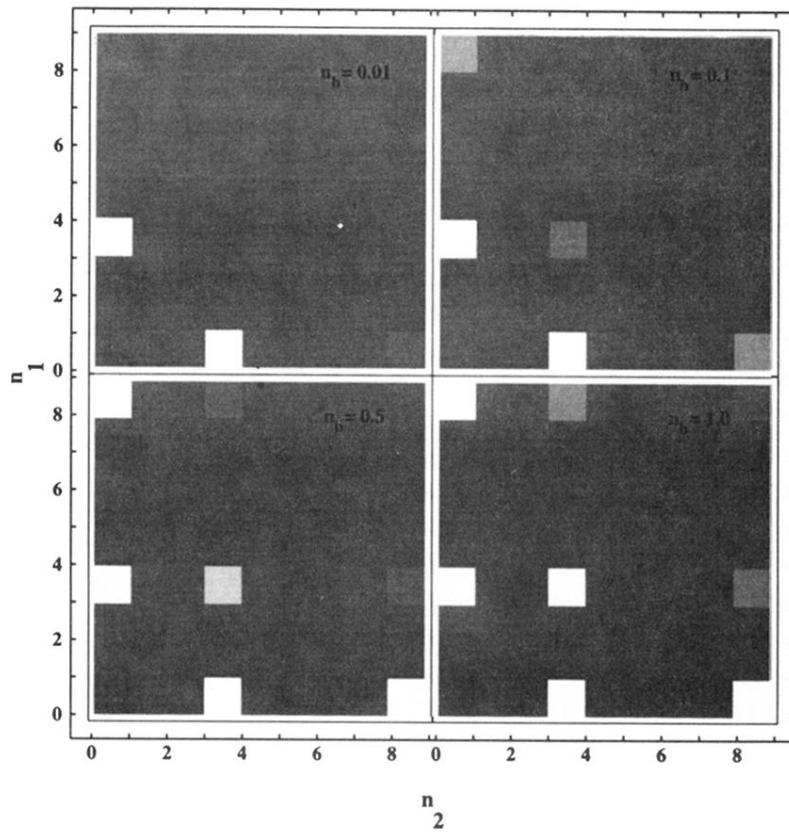


FIG. 12. Density plot of the photon statistics for four different values of the mean thermal photon number n_b that are given in the figure at cavity loss of $\gamma t = 0.0001$ and at atom number $k = 1000$. The initial state of the fields is the pure state, $|\Psi\rangle_0^{(1)}$, applying $g\tau = \pi$, the steady state of which would be $|\Psi\rangle_0^{(3)}$ in the absence of losses. New trapping states contribute due to the coupling between the blocks that were disconnected at zero temperature.

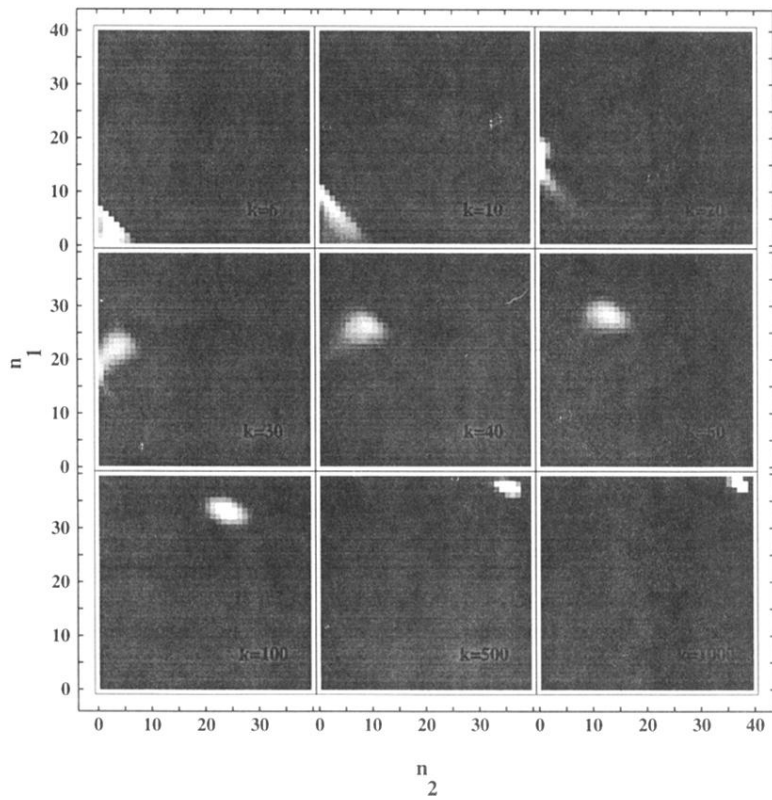


FIG. 3. Density plot of the time evolution of the photon statistics of the fields started from vacuum applying $g\tau=0.5$. Brighter points correspond to higher probabilities, the gray level to zero, and numbers k in the figure are the atom numbers. After an initial flip lasting until $k \cong 20$ the fields evolve toward $n_1 \cong n_2 \cong 38$ in a well-localized structure.

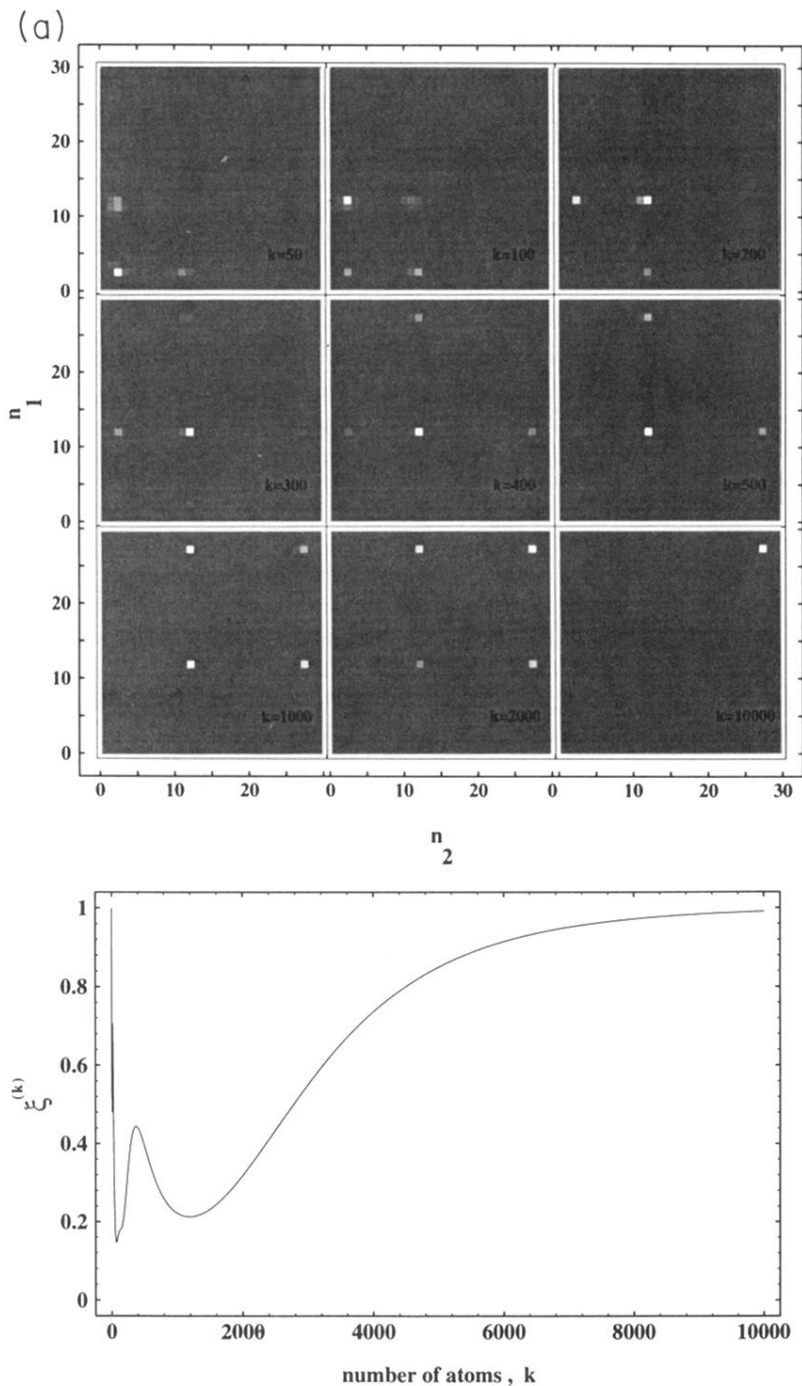


FIG. 4. (a) Density plot of the time evolution of the photon statistics of the fields started from vacuum applying $g\tau = 3\pi/\sqrt{29}$. The system spends long times in the pseudotrapping points around $N_1 \cong 2$ and $N_2 \cong 12$ and combinations thereof, until it finally evolves into the true-trapping point at $N_3 = 28$. (b) The evolution of the purity factor, $\xi^{(k)} = \text{Tr}[\rho^{(k)2}]$, as a function of the atom number k corresponding to the fields depicted in (a). The peak around $k \cong 400$ corresponds to photon statistics that are very similar to that of the number state, $|12, 12\rangle$, at the pseudotrapping point, $N_2 \cong 12$. Finally, the steady state is the number state, $|28, 28\rangle$, with purity factor of 1.

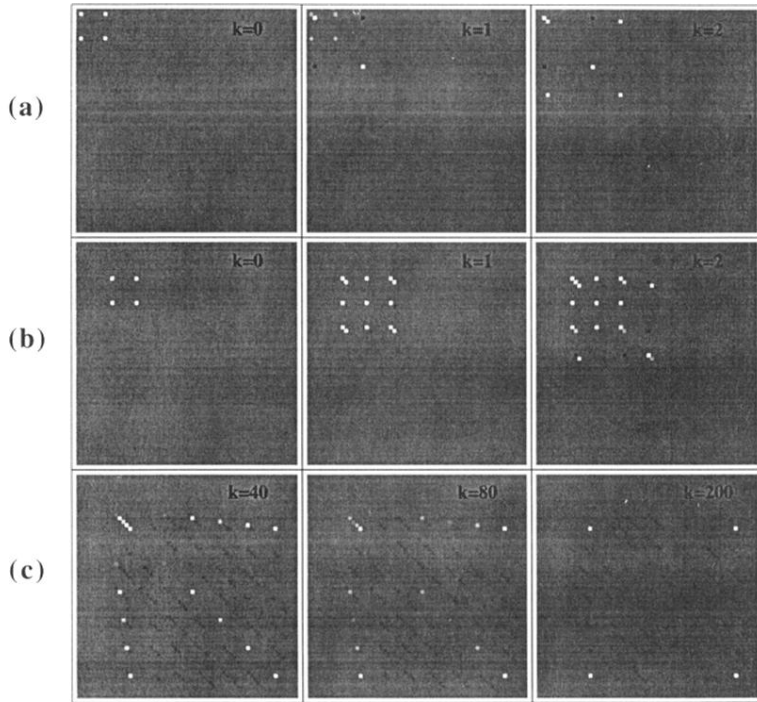


FIG. 5. Density plot of field-density matrices in the form of supermatrices discussed in Fig. 2 at atom numbers k given in the figure (dark points correspond to negative values). The initial states and applied $g\tau$'s are (a) $|\Psi\rangle_0^{(1)}$, $g\tau = \pi$, (b) $|\Psi\rangle_1^{(1)}$, $g\tau = \pi/\sqrt{2}$, and (c) $|\Psi\rangle_1^{(1)}$, $g\tau = 7\pi/\sqrt{2}$. The evolution of the density matrix shows statistical mixtures of pure states of (a) $|\Psi\rangle_0^{(m)}$ for $m = 1, 2, 3$ and (c) $|\Psi\rangle_1^{(m)}$ for $m = 1, \dots, 6$, resulting in pure steady states of (a) $|\Psi\rangle_0^{(3)}$ and (c) $|\Psi\rangle_1^{(6)}$. In the case of (b) other states of different structures also contribute, resulting in a mixed quantum state of the fields at steady state.

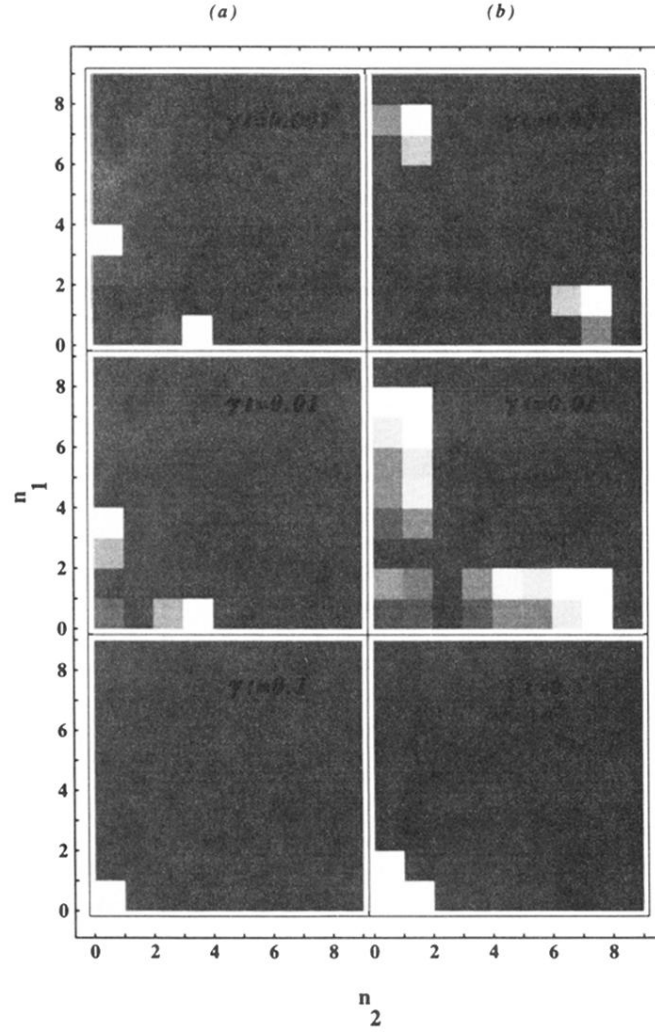


FIG. 9. Steady-state photon statistics of the fields started from the initial pure states (a) $|\Psi\rangle_0^{(1)}$, at $g\tau=\pi$ and (b) $|\Psi\rangle_1^{(1)}$, at $g\tau=7\pi/\sqrt{2}$ for three different losses of $\gamma t=0.001, 0.01$, and 0.1 given in the figure. In the case of small cavity losses the steady states of the fields are classical mixtures of the photon numbers (a) 0 and 3 and (b) 1 and 7, which spread out toward the vacuum for increasing losses.